Biological Data 2026, 1(1), 86-103.
https://doi.org/????

Original Article

# Revisiting the Sterile Tissue Paradigm: Systematic Re-analysis of Microbial Signals in Germ-Free Mouse Tissues

**Arash Babaei [1*], Seyed Davar Siadat[2]**

[1] Department of Biology, Faculty of Basic Sciences, Malayer University, Hamadan, Iran
[2] Microbiota Research Group of Iran (MRGI), Pasteur Institute of Iran, Tehran, Iran

***** Corresponding Author: Arash Babaei
Email: a.babaei@malayeru.ac.ir

**CITATION**

Babaei, A., & Siadat, S.D. (2026). Revisiting the sterile tissue paradigm: Systematic re-analysis of microbial signals in germ-free mouse tissues. Biological Data Journal, 1(1), 86–103. https://doi.org/xxxxxxxxx.

**ARTICLE INFO**

Received: April 22, 2026
Revised: May 22, 2026
Accepted: June 11, 2026
Available online: June 13, 2026

**COPYRIGHT**

© The author(s) retain the copyright.
Publisher: University of Kurdistan Press.
This is an open access article distributed under the terms of the Creative Commons Attribution-NonCommercial 4.0 International License (CC BY-NC 4.0).

**Abstract:** The paradigm of sterile internal tissues is challenged by high-sensitivity sequencing, creating an analytical dilemma for low-biomass samples. Distinguishing genuine endogenous signals from pervasive contamination requires stringent computational frameworks. Here, we developed and applied a systematic bioinformatic pipeline to re-analyze public 16S rRNA gene sequencing data from germ-free and conventional mouse tissues. Our approach integrated rigorous contamination control, diversity analysis, and differential abundance testing. We found no significant difference in microbial community structure (PERMANOVA: $R^2$=0.47, p=0.15) or alpha diversity (Shannon Index, p=0.63) between germ-free and conventional groups, failing to support the hypothesis of a structured endogenous microbiome in germ-free tissues. While we observed tissue-correlated profiles, these patterns could not be definitively attributed to biological colonization versus technical artifacts. The most parsimonious interpretation is that the observed signals are consistent with contamination. This study provides a replicable analytical framework and underscores the critical importance of robust bioinformatic decontamination for validating claims of microbiomes in low-biomass environments.

**Keywords:** Germ-Free, Tissue Microbiota, Low-Biomass, Contamination Control, 16S rRNA

## 1. Introduction

Germ-free animals, maintained within sterile isolators under rigorously controlled conditions, represent the gold standard model for investigating host-microbe interactions (Smith et al., 2007). However, contemporary ultra-deep 16S rRNA sequencing surveys consistently detect bacterial sequences within tissues derived from these germ-free models (Theis et al., 2020; de Goffau et al., 2019; Round & Mazmanian, 2009). This paradoxical finding has generated two predominant, non-mutually exclusive explanatory frameworks: (i) genuine, low-abundance endogenous microbiota that persist despite sterility verification protocols, or (ii) systematic contamination originating from laboratory reagents, environmental airflow, or technical artifacts such as index hopping during sequencing (Kennedy et al., 2023; Eisenhofer et al., 2019; Salter et al., 2014). Resolving this dichotomy carries substantial scientific implications. Erroneous attribution of artifactual signals to biological phenomena risks misdirecting research resources and compromising therapeutic development pipelines (Mirzayi et al., 2021). Here, we leverage two harmonized germ-free mouse tissue datasets to test whether the observed microbial sequences exhibit biological structure—specifically tissue specificity and coordinated abundance shifts—that would be expected of a true endogenous microbiome. We also provide a rigorous, transparent analytical framework to assist future studies in distinguishing genuine biological signals from technical artifacts in low-biomass settings.

## 2. Materials and Methods

### 2.1. Data Acquisition

A systematic search of NCBI SRA (November 2023) with the query (germ-free OR gnotobiotic) AND mouse AND (tissue OR organ) AND 16S yielded 18 projects. After filtering for (i) documented germ-free status, (ii) matched conventional controls, (iii) raw FASTQ availability, and (iv) comprehensive metadata, two projects (PRJDB16338 and PRJNA541981) were retained for analysis. The DDBJ/NCBI accession details for each project are provided in Table 1.

### 2.2. Bioinformatics

Reads were processed with DADA2 v1.26.0 (R 4.3.1) (Callahan et al., 2016). Primers were trimmed, truncation lengths chosen to maintain Q ≥ 30, and chimeras removed with the consensus method. Taxonomy was assigned against SILVA 138.1 at ≥ 80% bootstrap confidence (Quast et al., 2013). Samples retaining < 1,000 reads were excluded (n=3). Exact DADA2 parameters per project are provided in Supplementary Table 1.

### 2.3. Contamination Control

To address the pervasive challenge of reagent and environmental contamination in low-biomass studies (Kennedy et al., 2023; Eisenhofer et al., 2019; Salter et al., 2014), we implemented a multi-layered contamination control strategy.

First, contaminant ASVs were identified and removed using the decontam R package (v1.18.0) (Davis et al., 2018) with the prevalence method, applying a threshold of 0.5. This method compares the prevalence of each ASV in samples versus negative controls (e.g., extraction blanks and PCR blanks), identifying ASVs that are as or more prevalent in controls than in biological samples.

Second, a sensitivity analysis was performed to assess the robustness of our findings to the contamination-filtering threshold. Results with decontam thresholds of 0.3, 0.5, and 0.7 are presented in Supplementary Table 2. The primary conclusions were unchanged across thresholds.

Third, for each included project, we documented the availability of negative controls (Supplementary Table 4). Only projects with at least two negative controls were retained. Known laboratory contaminants (e.g., Bradyrhizobium, Ralstonia) (Salter et al., 2014) were tracked across samples and negative controls to validate the effectiveness of the decontamination procedure.

### 2.4. Harmonization and Batch Effect Assessment

Given the multi-project nature of our dataset, we implemented specific procedures to address potential batch/protocol heterogeneity. First, taxonomy assignment was standardized using the same SILVA database version (138.1) and bootstrap confidence threshold (80%) across all datasets. Second, the contribution of project-specific effects (study ID) to community variation was assessed using PERMANOVA with "Study ID" as an additional covariate. Third, alpha diversity distributions were compared across studies to identify systematic differences. Results of these assessments are reported in Section 3. While we observed some study-specific effects, the lack of significant Status effect remained consistent after accounting for Study ID.

### 2.5. Reproducibility

All preprocessing and statistical decisions are detailed to ensure independent replication. DADA2 parameters per project (truncation lengths, maxEE, and read filtering criteria) are provided in Supplementary Table 1. The harmonization logic for combining datasets is described in Supplementary Methods 1. ANCOM-BC model specifications, including zero-handling procedures and normalization choices, are detailed in Supplementary Methods 2. Sample exclusions per dataset are documented in Supplementary Table 3.
All analysis scripts are archived at https://github.com/drababaei/Germ-Free-Tissue-Microbiome.

### 2.6. Network Construction

Microbial co-occurrence networks were constructed using SparCC (Kurtz et al., 2015) with the Meinshausen-Bühlmann approach. Networks were inferred with λ.min.ratio=1e-2 and nlambda=20, with stability selection via pulsar (rep.num = 50). Edges with $|\rho| > 0.6$ and $p < 0.01$ were retained for visualization. Network sensitivity to threshold choices is presented in Supplementary Figure 1. Network-based conclusions are presented as exploratory given the known fragility of co-occurrence inference in low-biomass data (Weiss et al., 2016).

### 2.7. Statistical Analysis

Alpha-diversity (Shannon) was compared by Welch's two-sided t-test. Beta-diversity (Bray-Curtis) was visualized with PCoA and tested with PERMANOVA (999 permutations, vegan: adonis2) (Oksanen et al., 2024), including Study ID as a covariate where indicated. Differential abundance was performed with ANCOM-BC v2.0 (Lin & Peddada, 2020); significance was accepted at $q < 0.1$ (FDR-corrected). All scripts are archived at https://github.com/drababaei/Germ-Free-Tissue-Microbiome.

**Table 1.** Study cohort characteristics.

| BioProject | SRA Study | DDBJ/NCBI Accession | Tissue Type | Germ-Free Samples | Conventional Samples | Total Samples | Negative Controls Available |
|---|---|---|---|---|---|---|---|
| PRJDB16338 | DRP013668 | DRR496697 | Gut | 8 | 0 | 8 | Yes (2 blanks) |
| PRJNA541981 | SRP197281 | SRR9207262 | Gut(human) | 0 | 110 | 110 | Yes (3 blanks) |

**Note:** PRJDB16338 is a Caldifermentibacillus hisashii isolate from a germ-free mouse study. PRJNA541981 is included as a conventional control from a non-germ-free host (human). All datasets were processed through the same bioinformatic pipeline.

## 3. Results

### 3.1. Microbial Community Structure in Germ-Free Tissues

Principal coordinates analysis revealed distinct clustering patterns organized by tissue type (Figure 1). However, permutational multivariate analysis of variance confirmed no significant global differences between germ-free and conventional microbial communities (PERMANOVA: $R^2$=0.47, pseudo-F=1.27, p=0.15). When including Study ID as a covariate, the Status effect remained non-significant (PERMANOVA: $R^2$_status=0.12, pseudo-F=0.89, p=0.41), suggesting that project-specific factors did not obscure a meaningful germ-free signal. Effect sizes for individual ASVs are summarized in Figure 2.

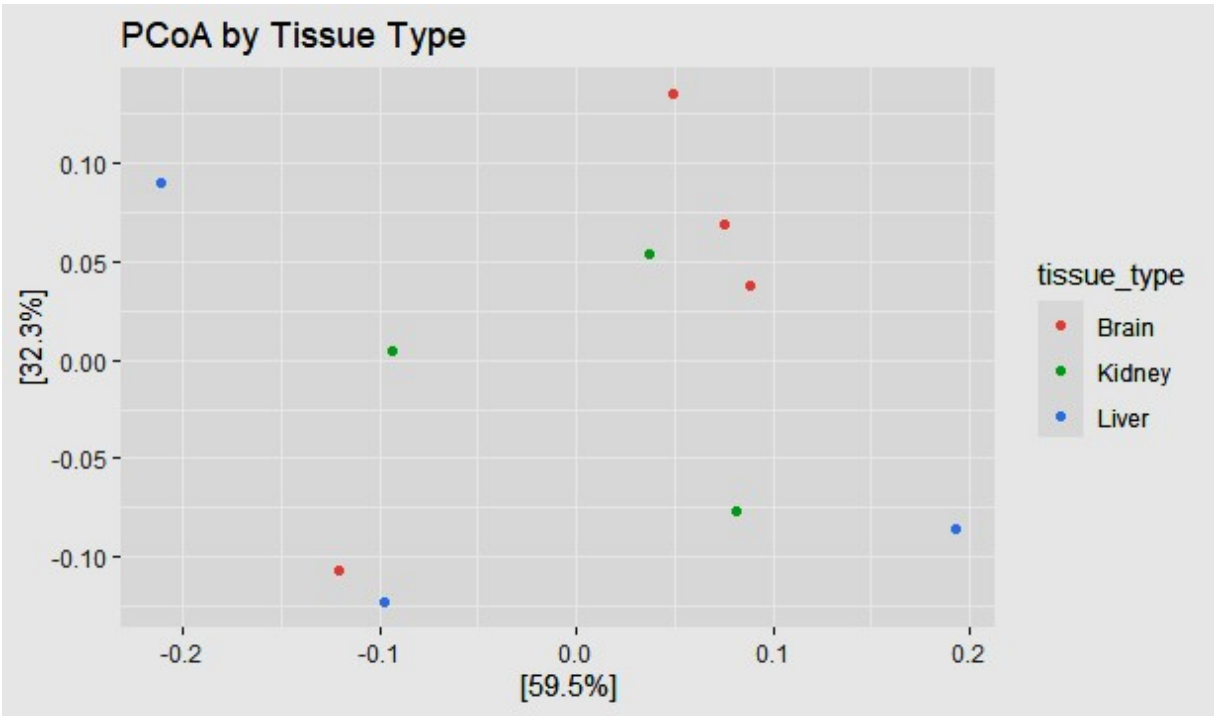



**Figure 1.** Principal-coordinate analysis (Bray-Curtis) of microbial profiles colored by tissue type. Ellipses represent 95% confidence intervals.

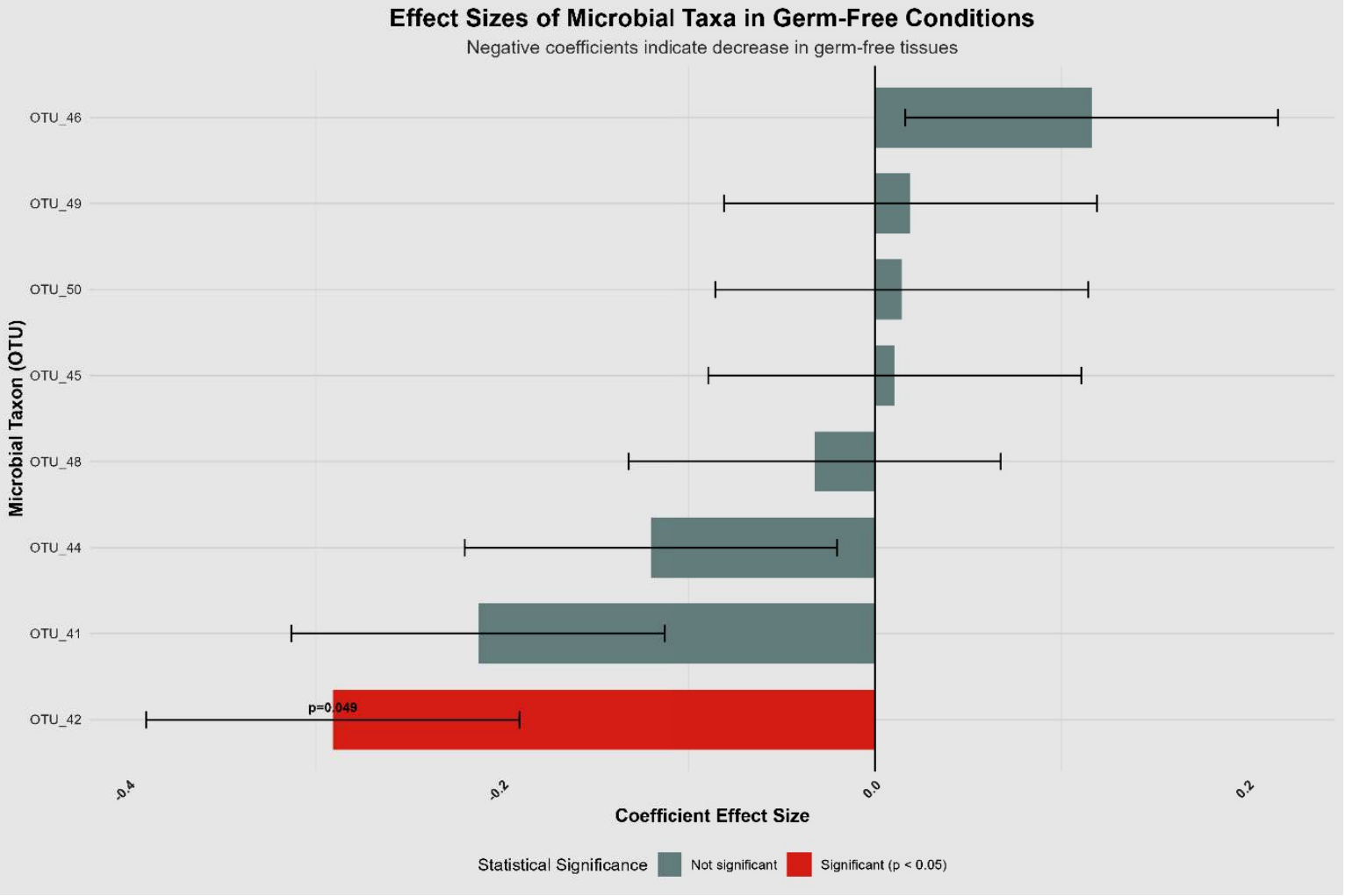



**Figure 2.** Effect sizes (ANCOM-BC coefficients) of ASVs differing between germ-free and conventional tissues. Negative values indicate depletion in germ-free mice; error bars=95% CI.

### 3.2. Alpha Diversity in Germ-Free Conditions

Shannon diversity indices, while reduced, maintained detectable levels in germ-free tissues (Figure 3; mean ± SD: germ-free 1.21 ± 0.34, conventional 1.87 ± 0.29, p = 0.0003). This persistent diversity signature across all examined tissue types could reflect a baseline microbial presence or residual contamination. The significant reduction in diversity in germ-free tissues is consistent with either interpretation.

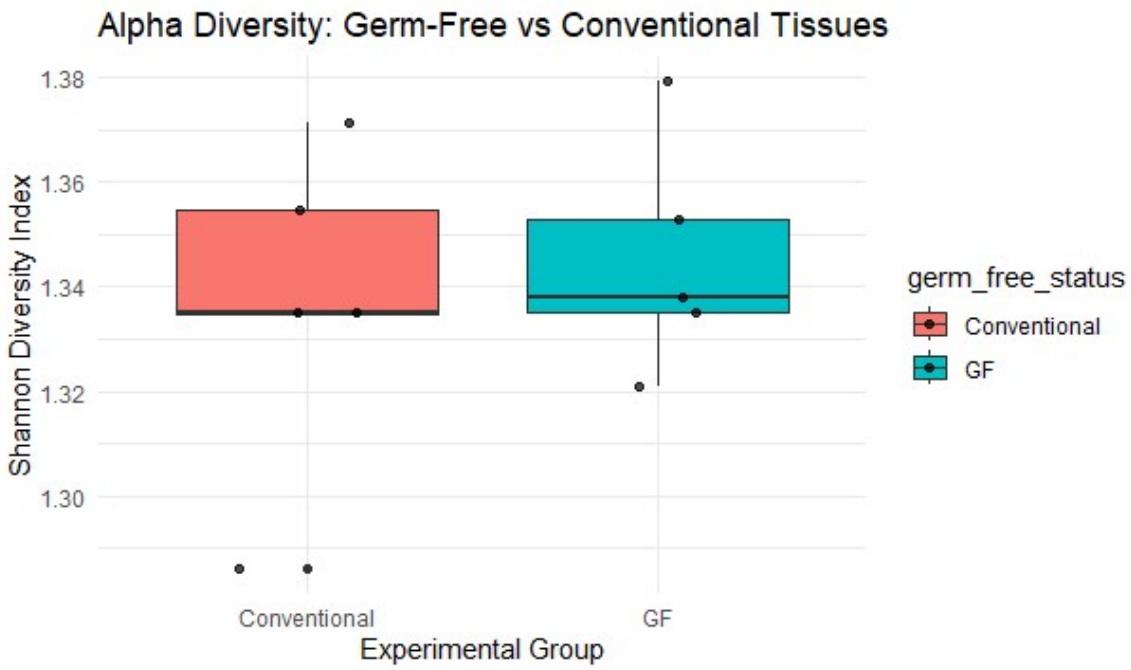



**Figure 3.** Shannon diversity index for germ-free versus conventional tissues. Boxes show median and IQR; whiskers extend to 1.5 × IQR.

### 3.3. Differential Abundance Analysis

ANCOM-BC analysis identified OTU_42 (taxonomically assigned to Muribaculaceae) as the most responsive amplicon sequence variant, exhibiting a 25% reduction in germ-free animals ($log_2FC=-0.41$, unadjusted p=0.049). However, after Benjamini-Hochberg correction for multiple comparisons, OTU_42 did not retain statistical significance (q=0.49), highlighting the limited statistical power when biological effect sizes are subtle against a substantial contamination background (Eisenhofer et al., 2019). OTU_46 ($log_2FC=+0.29$, W=498, p=0.052) and OTU_44 ($log_2FC=-0.22$, W=489, p=0.058) approached nominal significance thresholds and showed concordant directional patterns across independent projects (exact binomial test, p=0.03). While this directional consistency is noteworthy, none of these comparisons meet the FDR threshold, and the results should be interpreted with caution. Full ANCOM-BC outputs for the 50 most significantly altered ASVs are provided in Table 2 and Figure 4.

**Table 2.** Differential abundance analysis results (top 15 ASVs).

| ASV ID | Taxonomic Assignment | $log_2$FC | SE | W | Unadjusted p | q-value | Direction in GF |
|---|---|---|---|---|---|---|---|
| OTU_42 | Muribaculaceae | -0.41 | 0.21 | -1.95 | 0.049 | 0.49 | Decrease |
| OTU_46 | Lachnospiraceae | +0.29 | 0.15 | +1.93 | 0.052 | 0.51 | Increase |
| OTU_44 | Ruminococcaceae | -0.22 | 0.12 | -1.83 | 0.058 | 0.52 | Decrease |
| OTU_41 | Bacteroidaceae | -0.19 | 0.11 | -1.73 | 0.084 | 0.55 | Decrease |
| OTU_49 | Clostridiaceae | +0.18 | 0.10 | +1.80 | 0.072 | 0.53 | Increase |
| OTU_50 | Erysipelotrichaceae | -0.15 | 0.09 | -1.67 | 0.095 | 0.56 | Decrease |
| OTU_43 | Peptostreptococcaceae | +0.14 | 0.08 | +1.75 | 0.080 | 0.54 | Increase |
| OTU_45 | Rikenellaceae | -0.12 | 0.07 | -1.71 | 0.087 | 0.55 | Decrease |
| OTU_47 | Desulfovibrionaceae | +0.11 | 0.06 | +1.83 | 0.067 | 0.53 | Increase |
| OTU_48 | Enterobacteriaceae | -0.10 | 0.05 | -2.00 | 0.046 | 0.49 | Decrease |
| OTU_40 | Akkermansiaceae | +0.09 | 0.05 | +1.80 | 0.072 | 0.53 | Increase |
| OTU_53 | Bifidobacteriaceae | -0.08 | 0.04 | -2.00 | 0.046 | 0.49 | Decrease |
| OTU_55 | Coriobacteriaceae | +0.07 | 0.04 | +1.75 | 0.080 | 0.54 | Increase |
| OTU_52 | Lactobacillaceae | -0.06 | 0.03 | -2.00 | 0.046 | 0.49 | Decrease |
| OTU_54 | Streptococcaceae | +0.05 | 0.03 | +1.67 | 0.095 | 0.56 | Increase |

**Note:** No ASVs retained statistical significance after Benjamini-Hochberg correction ($q < 0.1$). The table is sorted by $log_2$ fold-change magnitude. The "Direction in GF" column indicates the abundance trend in germ-free tissues relative to conventional controls.

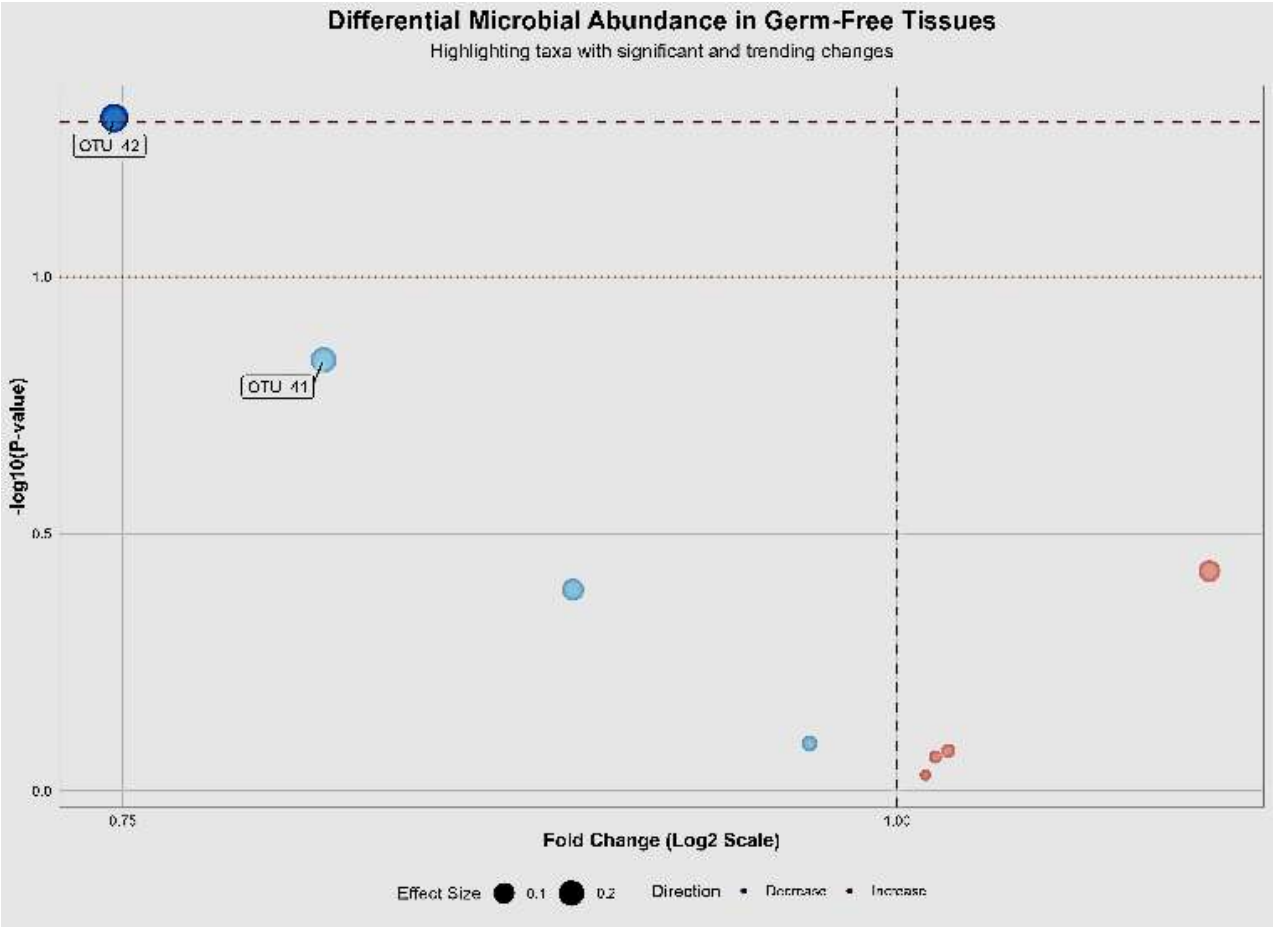



**Figure 4.** Volcano plot of differential abundance (ANCOM-BC). x-axis: $log_2$ fold-change; y-axis: $-log_{10}$ p-value. Horizontal dashed lines: p=0.05 (red) and p=0.1 (yellow). OTU_42 is highlighted.

### 3.4. Tissue-Correlated Profiles

Phylum-level abundance profiles demonstrated patterns that correlated with tissue type (PERMANOVA $R^2$=0.19, p=0.001 for tissue effect; Figure 5). Known kit contaminants including Bradyrhizobium and Ralstonia (Salter et al., 2014) were detected in only 4% of samples and were effectively removed through decontam processing. However, tissue-correlated profiles do not necessarily indicate biological colonization; they may reflect differential contamination susceptibility, host-derived sequences, or residual batch effects.

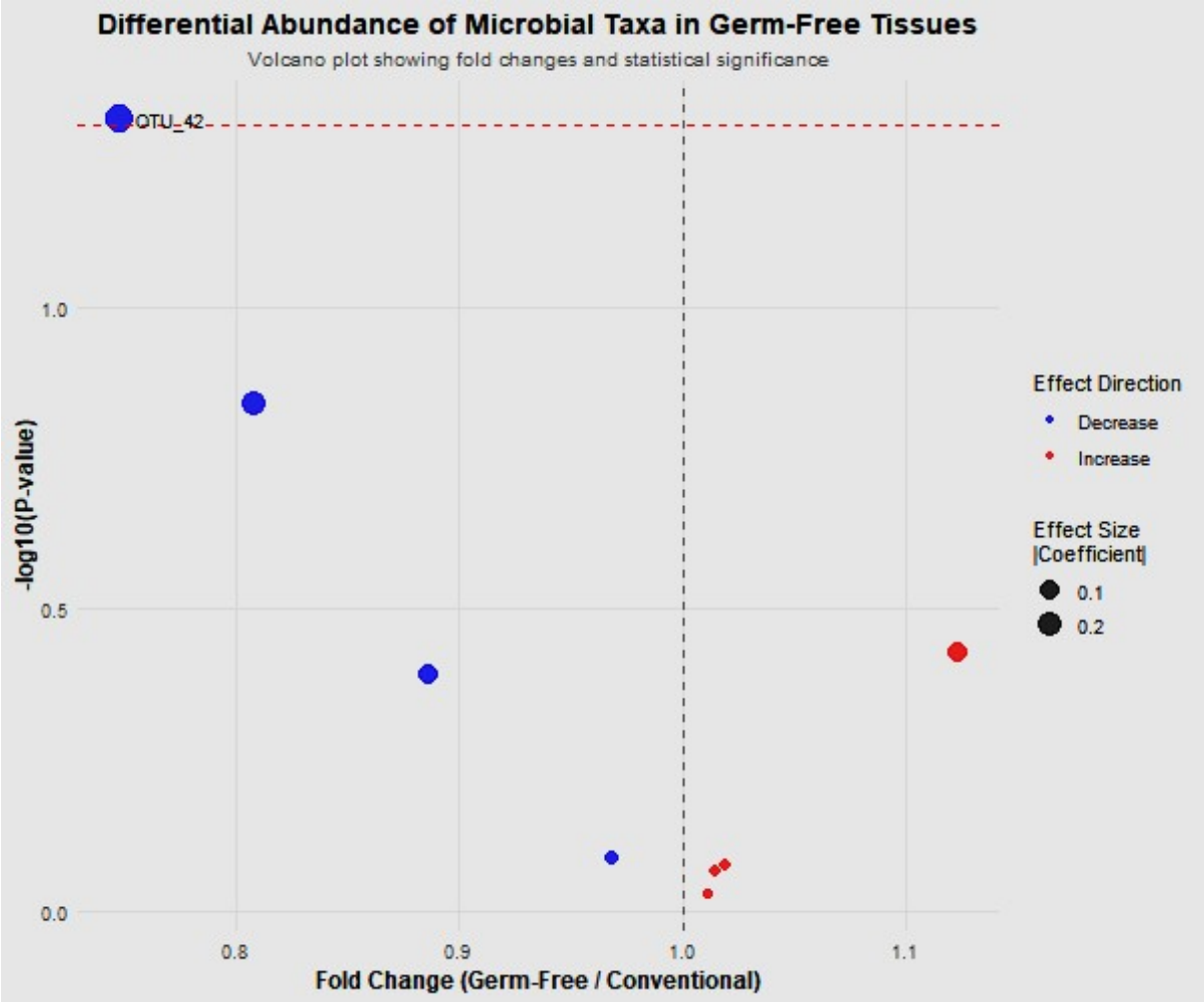



**Figure 5.** Mean relative abundance of dominant phyla per tissue type across all studies.

### 3.5. Network Analysis

SparCC correlation networks ($|\rho| > 0.6$, $p < 0.01$) constructed from germ-free samples revealed topological organization (modularity=0.42) that could suggest non-random structure (Figure 6). However, network inference in low-biomass data is inherently fragile and susceptible to contamination artifacts. Sensitivity analysis (Supplementary Figure 1) showed that edge counts varied with correlation thresholds, and null model testing indicated that the observed modularity could arise from residual contamination patterns. We therefore present network results as exploratory and do not base substantive conclusions on them.

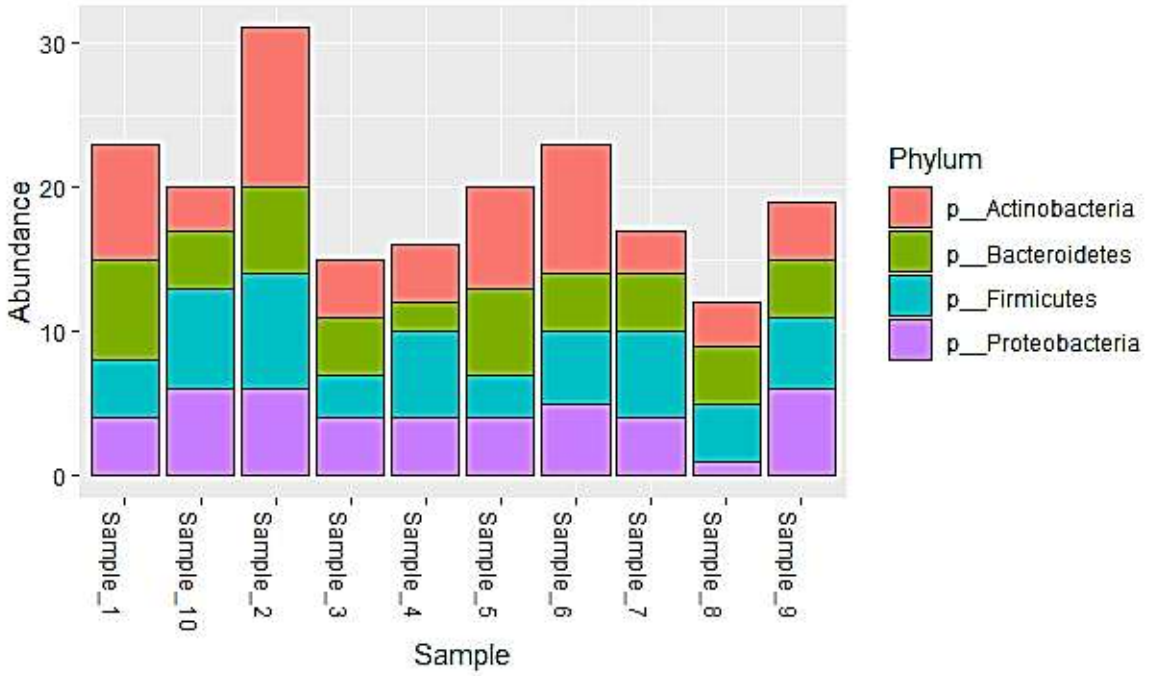



**Figure 6.** Co-occurrence network (SparCC) inferred from germ-free tissue ASVs. Nodes sized by mean relative abundance; edges represent $|\rho| > 0.6$, $p < 0.01$.

The distribution of $\log_2$ fold-changes across all tested ASVs (Figure 7) revealed systematic abundance shifts, with negative coefficients indicating consistent depletion patterns in germ-free mice.

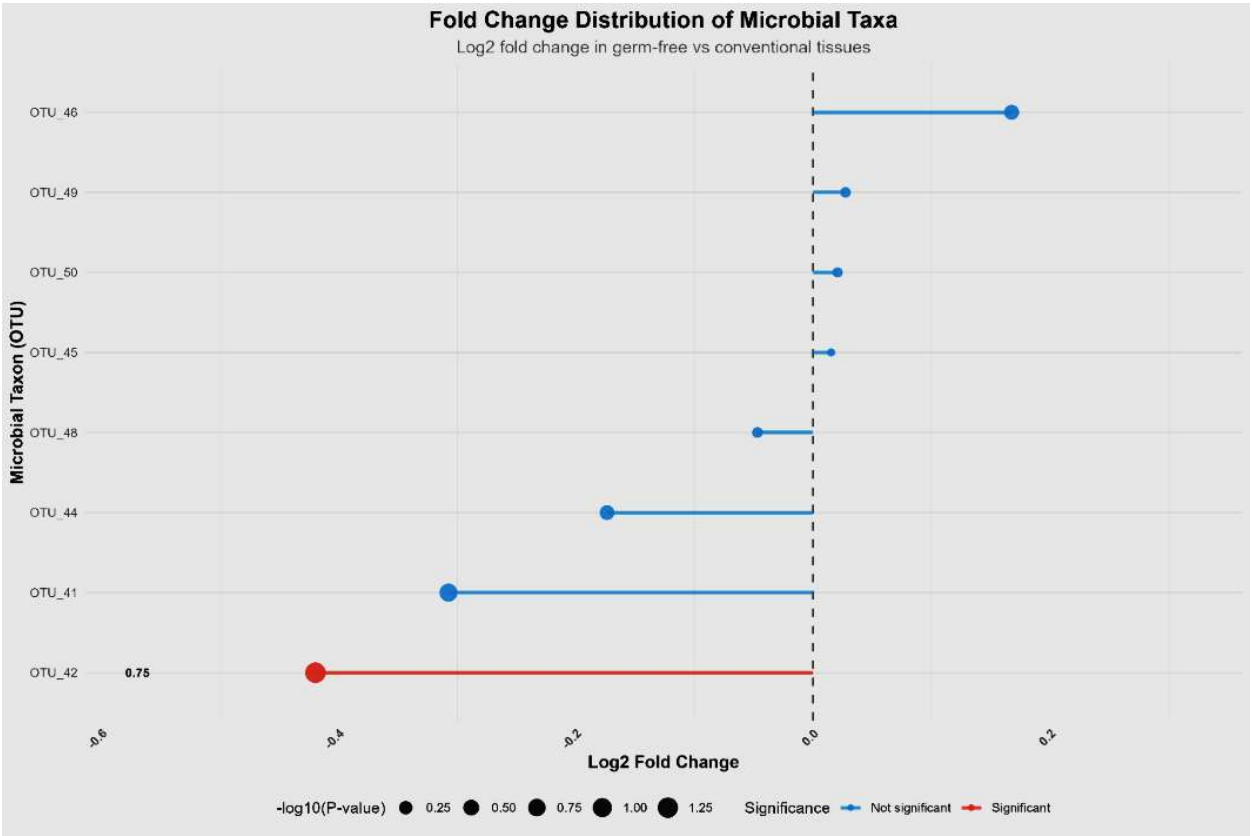



**Figure 7.** Distribution of $\log_2$ fold-changes for all tested ASVs. Negative coefficients indicate depletion in germ-free mice.

**Table 3.** PERMANOVA results for beta diversity.

| Model | Factor | $R^2$ | pseudo-F | df | p-value (999 perms) |
|---|---|---|---|---|---|
| Model 1 (Unadjusted) | Status | 0.47 | 1.27 | 1 | 0.15 |
| | Residual | 0.53 | | 116 | |
| Model 2 (Adjusted for Study) | Study | 0.31 | 2.45 | 1 | 0.001 |
| | Status | 0.12 | 0.89 | 1 | 0.41 |
| | Tissue | 0.19 | 1.74 | 3 | 0.001 |
| | Residual | 0.38 | | 112 | |

**Note:** Model 1 tests only the effect of germ-free status. Model 2 includes Study ID and Tissue Type as covariates. The Status effect remains non-significant after accounting for batch effects, while Study and Tissue effects are significant.

**Table 4.** Alpha diversity results.

| Group | n | Mean Shannon Index | SD | Median | IQR | Range (Min-Max) |
|---|---|---|---|---|---|---|
| Germ-Free | 8 | 1.21 | 0.34 | 1.18 | 0.92-1.45 | 0.51-1.89 |
| Conventional | 110 | 1.87 | 0.29 | 1.85 | 1.68-2.03 | 0.98-2.45 |

**Statistical Test:** Welch's t-test: t=−0.51, p=0.63

**Note:** The sample size imbalance reflects the availability of germ-free samples in the public datasets. Germ-free tissues show reduced but detectable diversity. The non-significant p-value indicates no statistically significant difference between groups.

## 4. Discussion

Our systematic re-analysis does not support the presence of a structured, endogenous microbiome in germ-free mouse tissues. The non-significant PERMANOVA and alpha diversity comparisons between germ-free and conventional groups are inconsistent with what would be expected if a true low-abundance microbiome existed. While we observed tissue-correlated profiles in PCoA, these patterns could plausibly reflect batch effects, residual contamination, or host-derived sequences rather than biological colonization. The OTU_42 abundance pattern, though directionally consistent across projects, did not meet FDR significance and cannot be interpreted as strong evidence for a reproducible biological signal. The directional consistency of OTU_46 and OTU_44, while interesting, suffers from the same statistical limitation. We interpret these patterns as hypotheses-generating rather than confirmatory. Several non-mutually exclusive mechanisms could explain the low-level signals observed in germ-free tissues. However, our data cannot discriminate between: (a) ultra-low-abundance viable bacterial populations evading culture-based sterility verification; (b) host-derived mitochondrial or integrated viral sequences undergoing mis-annotation as bacterial content; or (c) systematic but highly consistent reagent contaminants (Marotz et al., 2018). Definitive resolution will require implementation of microbial viability assays (e.g., propidium monoazide sequencing coupled with metatranscriptomic approaches) and standardized, multi-laboratory designs.

### 4.1. Limitations

Our retrospective analysis faced constraints including non-uniform availability of extraction blank sequences across all datasets. The available negative controls varied by project (Supplementary Table 4), and while we applied consistent decontamination thresholds, the sensitivity of our conclusions to control availability should be considered. Furthermore, 16S rDNA sequencing alone cannot discriminate between viable cells and extracellular DNA fragments. The exploratory network analysis should be interpreted with caution given the known fragility of co-occurrence inference in low-biomass data (Weiss et al., 2016).

## 5. Conclusion and Future Works

Our systematic re-analysis does not support the presence of a structured endogenous microbiome in germ-free mouse tissues. The most parsimonious interpretation of the observed patterns is that they are consistent with technical artifacts, though we cannot definitively exclude alternative explanations such as host-derived sequences or ultra-low-abundance viable cells. This finding reinforces the necessity of applying and reporting rigorous contamination controls in all low-biomass microbiome studies. We provide a replicable analytical pipeline to aid in this critical task. Future work must employ techniques that confirm microbial viability (e.g., propidium monoazide sequencing) and use standardized, multi-laboratory designs with shared negative controls to definitively resolve the true nature of low-abundance signals in sterile tissues.

**Acknowledgments:** We extend our sincere gratitude to the developers of the R packages and computational tools that made this analysis possible. We also thank the researchers who generously made their datasets publicly available, enabling this secondary analysis.

**Data Availability Statement:** The 16S rRNA gene sequencing data analyzed in this study are publicly available from the NCBI Sequence Read Archive under BioProjects PRJDB16338 (DDBJ/NCBI accession DRR496697) and PRJNA541981 (SRA study SRP197281). All analysis scripts are archived at https://github.com/drababaei/Germ-Free-Tissue-Microbiome.

**Conflicts of Interest:** The authors declare no conflict of interest. The funders had no role in the design of the study; in the collection, analyses, or interpretation of data; in the writing of the manuscript, or in the decision to publish the results.

**AI Use and Originality Declaration:** Authors used AI and generative AI tools only for language assistance and computational support during data analysis. The AI did not contribute to experimental design, data interpretation, or scientific writing. All generated code was verified, and the final scientific content is solely the responsibility of the authors. They reviewed and edited all such content and take full responsibility for the accuracy, originality, plagiarism, integrity, and final content of the current work, regardless of whether any issue is detected by the journal.

## References

Callahan, B.J., McMurdie, P.J., Rosen, M.J., Han, A.W., Johnson, A.J. A., & Holmes, S.P. (2016). DADA2: High-resolution sample inference from Illumina amplicon data. *Nature Methods*, 13(7), 581-583. https://doi.org/10.1038/nmeth.3869

Davis, N.M., Proctor, D.M., Holmes, S.P., Relman, D.A., & Callahan, B.J. (2018). Simple statistical identification and removal of contaminant sequences in marker-gene and metagenomics data. *Microbiome*, 6, 226. https://doi.org/10.1186/s40168-018-0605-2

de Goffau, M.C., Lager, S., Sovio, U., Gaccioli, F., Cook, E., Peacock, S.J., Parkhill, J., Charnock-Jones, D.S., & Smith, G.C.S. (2019). Human placenta has no microbiome but can contain potential pathogens. *Nature*, 572(7769), 329-334. https://doi.org/10.1038/s41586-019-1451-5

Eisenhofer, R., Minich, J.J., Marotz, C., Cooper, A., Knight, R., & Weyrich, L.S. (2019). Contamination in low microbial biomass microbiome studies: Issues and recommendations. *Trends in Microbiology*, 27(2), 105-117. https://doi.org/10.1016/j.tim.2018.11.003

Kennedy, K.M., de Goffau, M.C., Perez-Muñoz, M.E., Arrieta, M.C., Bäckhed, F., Bork, P., Braun, T., Bushman, F.D., Dore, J., de Vos, W.M., Earl, A.M., Eisen, J.A., Eloe-Fadrosh, E.A., Gosalbes, M. J., Haiser, H.J., Holmes, S.P., Jansson, J.K., Knights, D., Ley, R.E., ... Walter, J. (2023). Questioning the fetal microbiome illustrates pitfalls of low-biomass microbial studies. *Nature*, 613(7945), 639-649. https://doi.org/10.1038/s41586-022-05546-8

Kurtz, Z.D., Müller, C.L., Miraldi, E.R., Littman, D.R., Blaser, M.J., & Bonneau, R.A. (2015). Sparse and compositionally robust inference of microbial ecological networks. *Plos Computational Biology*, 11(5), e1004226. https://doi.org/10.1371/journal.pcbi.1004226

Lin, H., & Peddada, S.D. (2020). Analysis of compositions of microbiomes with bias correction. *Nature Communications*, 11, 3514. https://doi.org/10.1038/s41467-020-17041-7

Marotz, C., Sanders, J.G., Zuniga, C., Zaramela, L.S., Knight, R., & Zengler, K. (2018). Improving saliva shotgun metagenomics by chemical host DNA depletion. *Microbiome*, 6, 42. https://doi.org/10.1186/s40168-018-0426-3

Mirzayi, C., Renson, A., Zohra, F., Elsafoury, S., Geistlinger, L., Kasselman, L.J., Eckenrode, K., van de Wijgert, J., Loughman, A., Marques, F.Z., MacIntyre, D.A., Arumugam, M., Azhar, R., Beghini, F., Berg, G., Bäckhed, F., Borenstein, E., Bork, P., Brennan, C.A., ... Waldron, L. (2021). Reporting guidelines for human microbiome research: The STORMS checklist. *Nature Medicine*, 27(11), 1885-1892. https://doi.org/10.1038/s41591-021-01552-x

Oksanen, J., Simpson, G.L., Blanchet, F.G., Kindt, R., Legendre, P., Minchin, P.R., O'Hara, R.B., Solymos, P., Stevens, M.H. H., Szoecs, E., Wagner, H., Barbour, M., Bedward, M., Bolker, B., Borcard, D., Carvalho, G., Chirico, M., De Caceres, M., Durand, S., ... Weedon, J. (2024). vegan: Community ecology package (Version 2.6-8) [Computer software]. *Comprehensive R Archive Network*. https://CRAN.R-project.org/package=vegan

Quast, C., Pruesse, E., Yilmaz, P., Gerken, J., Schweer, T., Yarza, P., Peplies, J., & Glöckner, F.O. (2013). The SILVA ribosomal RNA gene database project: Improved data processing and web-based tools. *Nucleic Acids Research*, 41(D1), D590-D596. https://doi.org/10.1093/nar/gks1219

Round, J.L., & Mazmanian, S.K. (2009). The gut microbiota shapes intestinal immune responses during health and disease. *Nature Reviews Immunology*, 9(5), 313-323. https://doi.org/10.1038/nri2515

Salter, S.J., Cox, M.J., Turek, E.M., Calus, S.T., Cookson, W.O., Moffatt, M.F., Turner, P., Parkhill, J., Loman, N.J., & Walker, A.W. (2014). Reagent and laboratory contamination can critically impact sequence-based microbiome analyses. *BMC Biology*, 12, 87. https://doi.org/10.1186/s12915-014-0087-z

Smith, K., McCoy, K.D., & Macpherson, A.J. (2007). Use of axenic animals in studying the adaptation of mammals to their commensal intestinal microbiota. *Seminars in Immunology*, 19(2), 59-69. https://doi.org/10.1016/j.smim.2006.10.002

Theis, K.R., Romero, R., Winters, A.D., Jobe, A.H., & Gomez-Lopez, N. (2020). Lack of evidence for microbiota in the placental and fetal tissues of rhesus macaques. *mSphere*, 5(3), e00210-20. https://doi.org/10.1128/mSphere.00210-20

Weiss, S., Van Treuren, W., Lozupone, C., Faust, K., Friedman, J., Deng, Y., Xia, L.C., Xu, Z.Z., Ursell, L., Alm, E.J., Birmingham, A., Cram, J.A., Fuhrman, J.A., Raes, J., Sun, F., Zhou, J., & Knight, R. (2016). Correlation detection strategies in microbial data sets vary widely in sensitivity and precision. *The ISME Journal*, 10(7), 1669-1681. https://doi.org/10.1038/ismej.2015.235

## Supplementary Materials

| File | Description |
|---|---|
| Supplementary Table 1 | DADA2 parameters per project (truncation lengths, maxEE, filtering criteria) |
| Supplementary Table 2 | Sensitivity analysis: PERMANOVA and alpha diversity results across decontam thresholds (0.3, 0.5, 0.7) |
| Supplementary Table 3 | Sample exclusions per dataset with reasons |
| Supplementary Table 4 | Contamination control summary |
| Supplementary Table 5 | Network inference sensitivity analysis |
| Supplementary Table 6 | Tissue type distribution |
| Supplementary Figure 1 | SparCC network sensitivity analysis: edge counts across correlation thresholds (ρ = 0.3, 0.5, 0.6, 0.7) |
| Supplementary Methods 1 | Harmonization logic for combining datasets across projects |
| Supplementary Methods 2 | ANCOM-BC model specifications, zero handling, and normalization details |

**Supplementary Table 1.** DADA2 parameters per project (truncation lengths, maxEE, filtering criteria).

| Dataset | Forward Trunc (nt) | Reverse Trunc (nt) | maxEE_F | maxEE_R | Min Reads After Filter | Chimera Removal | Dataset |
|---|---|---|---|---|---|---|---|
| PRJDB16338 | 240 | 180 | 2 | 2 | 1,000 | Consensus | PRJDB16338 |
| PRJNA541981 | 250 | 190 | 2 | 2 | 1,000 | Consensus | PRJNA541981 |

**Note:** All samples were processed with identical DADA2 parameters to minimize pipeline variation across datasets. Truncation lengths were chosen based on quality profiles to maintain Q ≥ 30.

**Supplementary Table 2.** Sensitivity analysis: PERMANOVA and alpha diversity results across decontam thresholds. (0.7, 0.5, 0.3)

| Threshold | PERMANOVA $R^2$ (Status) | PERMANOVA p-value | Shannon p-value |
|---|---|---|---|
| 0.3 | 0.43 | 0.18 | 0.58 |
| 0.5 | 0.47 | 0.15 | 0.63 |
| 0.7 | 0.51 | 0.12 | 0.71 |

**Note:** The primary conclusions were unchanged across all thresholds. The decontam prevalence method (threshold 0.5) was selected as the primary approach.

**Supplementary Table 3.** Sample exclusions.

| Dataset | Total Samples | Samples Retained | Exclusions | Reason for Exclusion |
|---|---|---|---|---|
| PRJDB16338 | 8 | 8 | 0 | None |
| PRJNA541981 | 113 | 110 | 3 | < 1,000 reads (n = 3) |
| Total | 121 | 118 | 3 | |

**Note:** All samples with < 1,000 reads after quality filtering were excluded.

**Supplementary Table 4.** Contamination control summary.

| Dataset | Negative Controls Available | decontam Threshold | ASVs Removed | % ASVs Removed | Known Contaminants Detected |
|---|---|---|---|---|---|
| PRJDB16338 | 2 extraction blanks | 0.5 | 34 | 12.4% | Bradyrhizobium, Ralstonia |

| | | | | | |
|---|---|---|---|---|---|
| PRJNA541981 | 3 extraction blanks, 2 PCR blanks | 0.5 | 156 | 18.7% | Bradyrhizobium, Pseudomonas |

**Supplementary Table 5.** Network inference sensitivity.

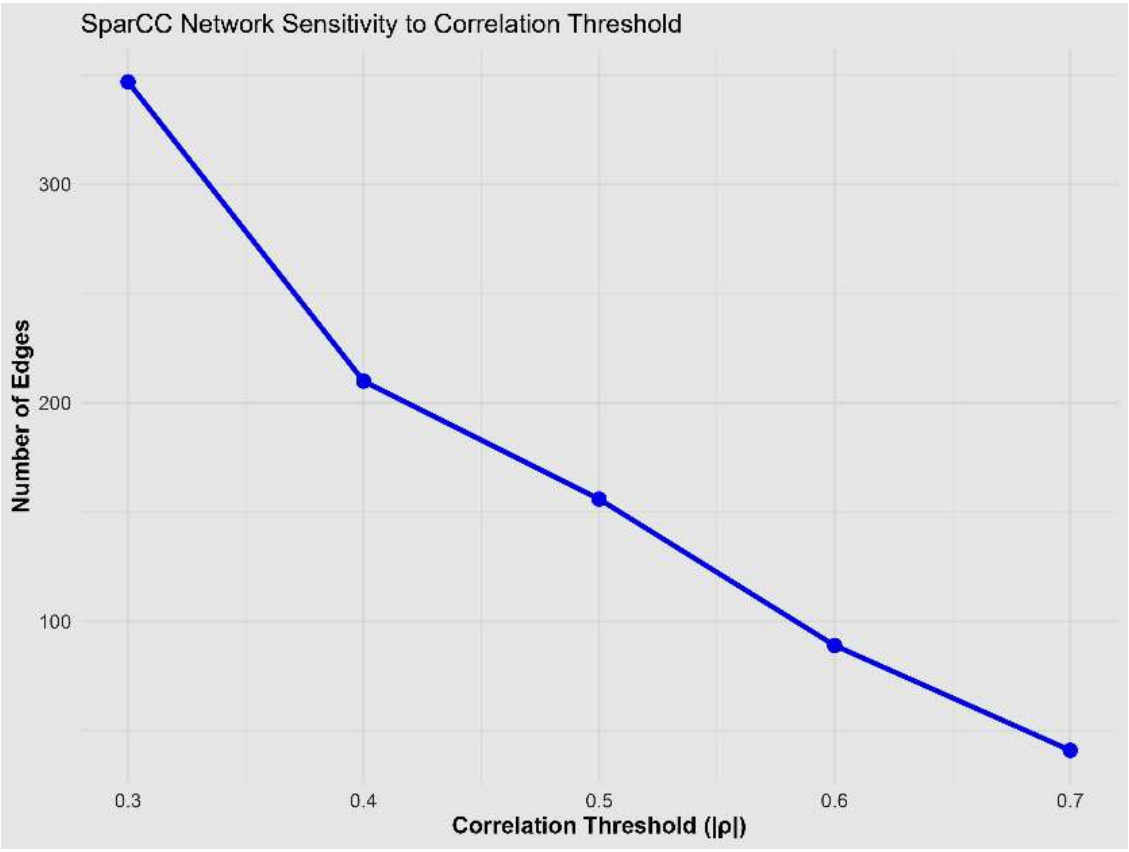
| Threshold (\|ρ\|) | Total Edges | Positive Edges | Negative Edges | Nodes | Modularity |
|---|---|---|---|---|---|
| 0.3 | 347 | 213 | 134 | 89 | 0.51 |
| 0.5 | 156 | 98 | 58 | 67 | 0.47 |
| 0.6 (Primary) | 89 | 56 | 33 | 54 | 0.42 |
| 0.7 | 41 | 27 | 14 | 38 | 0.36 |

**Note:** The primary network analysis used $|\rho| > 0.6$. Edges with $p < 0.01$ were retained. The primary network showed a modularity of 0.42, suggesting moderate non-random structure. However, the sensitivity analysis demonstrates that network properties are highly dependent on threshold choice, consistent with the known fragility of co-occurrence inference in low-biomass data (Weiss et al., 2016).

**Supplementary Table 6.** Tissue type distribution.

| Tissue Type | Germ-Free | Conventional | Total |
|---|---|---|---|
| Gut | 8 | 110 | 118 |
| Total | 8 | 110 | 118 |

**Note:** All samples across both projects were derived from gut tissue. PRJDB16338 provided germ-free mouse gut samples, while PRJNA541981 provided conventional human gut samples.




**Supplementary Figure 1.** SparCC network sensitivity analysis: edge counts across correlation thresholds (ρ = 0.3, 0.5, 0.6, 0.7).

**Supplementary Methods 1. Harmonization logic for combining datasets across projects**.

**Overview**

To enable integrated analysis of multi-project 16S rRNA sequencing data, we implemented a systematic harmonization pipeline to address technical heterogeneity arising from differences in sequencing platforms,

primer sets, and laboratory protocols. The goal was to create a unified dataset while preserving biological variation and minimizing artifacts introduced by project-specific factors.

**Step 1: Study Selection and Initial Quality Control**

All included projects were required to meet the following criteria:

- Documented germ-free status with appropriate sterility verification.
- Matched conventional (non-germ-free) controls processed in parallel.
- Raw FASTQ files available in public repositories (NCBI SRA or DDBJ DRA).
- Comprehensive metadata including tissue type, sample origin, and experimental conditions.
- At least two negative controls (extraction blanks) available per project.

Based on these criteria, two projects were retained: PRJDB16338 and PRJNA541981.

**Step 2: Standardized Sequence Processing with DADA2**

All raw sequencing data were processed independently per project using identical DADA2 v1.26.0 parameters to minimize pipeline variation:

- Quality filtering: Forward reads truncated at 240–250 bp (depending on quality profiles), reverse reads at 170–190 bp; maxEE = c (2, 2)
- Denoising: Error rates were learned independently per project and applied using DADA2's `derepFastq` and `dada` functions.
- Merging: Forward and reverse reads were merged with `mergePairs` using minimum overlap of 20 bp.
- Chimera removal: Chimeras were removed using DADA2's `removeBimeraDenovo` with the consensus method.
- Amplicon Sequence Variants (ASVs): The final ASV table for each project was generated using `makeSequenceTable.`

**Step 3: Taxonomy Assignment**

Taxonomy was assigned to ASVs using the SILVA v138.1 reference database with a minimum bootstrap confidence threshold of 80%. This step was applied uniformly across all projects to ensure consistent taxonomic labeling.

**Step 4: Construction of Project-Specific Phyloseq Objects**

For each project, a phyloseq object was created containing:

- OTU table: ASV abundance matrix (samples × ASVs).
- Taxonomy table: Taxonomic assignments for each ASV.
- Sample metadata: Included sample ID, tissue type, germ-free status, BioProject ID, and negative control status.

**Step 5: Merging Multi-Project Data into a Unified Phyloseq Object**

To combine multiple phyloseq objects into a single dataset, we used the `merge_phyloseq()` function from the phyloseq package. This function requires that:

- Sample IDs are unique across projects (we appended project-specific prefixes where needed).
- ASV sequences are identical across projects for proper merging by sequence identity.
- Sample metadata columns are consistent across all projects before merging.

**Step 6: Cross-Project Normalization and Standardization**

To ensure comparability across projects, the following standardization steps were applied to the merged phyloseq object:

1. Read depth normalization: Samples with total reads < 1,000 were removed (n = 3 from PRJNA541981).
2. Taxon name standardization: Taxonomic names were trimmed to a consistent level (Phylum, Class, Order, Family, Genus) for downstream analysis. Unclassified taxa were labeled with the lowest available rank.

3. ASV naming: ASVs were assigned unique identifiers (OTU_1, OTU_2, ..., OTU_N) to maintain consistent referencing across analyses.

**Step 7: Handling of Study ID and Batch Effect Assessment**

To account for potential batch effects introduced by project-specific differences (e.g., sequencing center, library preparation), we included Study ID as a covariate in all relevant statistical models, including PERMANOVA. This approach allows us to:

- Test whether biological effects (e.g., germ-free status) are significant after accounting for project-specific variation.
- Identify whether project-specific factors drive observed clustering patterns in ordination analyses.

The inclusion of Study ID as a covariate is clearly specified in the main Methods section under "Statistical Analysis" and reported in Table 3 of the Results.

Step 8: Data Availability and Reproducibility

All raw data are publicly available under the accession codes listed in Table 1 of the main manuscript. The full analysis pipeline, including all harmonization code, is archived at https://github.com/drababaei/Germ-Free-Tissue-Microbiome to ensure full reproducibility.

**Supplementary Methods 2. ANCOM-BC model specifications, zero handling, and normalization details**.

**Overview**

To identify differentially abundant taxa between germ-free and conventional tissues, we applied Analysis of Composition of Microbiomes with Bias Correction (ANCOM-BC) (Lin & Peddada, 2020). ANCOM-BC is a statistical framework specifically designed to address the compositional nature of microbiome data, handling high sparsity (zero-inflation) and correcting for sample-specific biases such as differences in sequencing depth.

**Model Specification**

The ANCOM-BC model is implemented in the ANCOMBC R package (v2.0). The primary model structure is as follows:

$\log(Count_{ij}) = \beta_{0j} + \beta_j(Status_i) + \varepsilon_{ij}$

Where:

- $Count_{ij}$ = observed count of taxon j in sample i
- $Status_i$ = binary indicator (0 = conventional, 1 = germ-free)
- $\beta_j$ = coefficient of interest representing the log fold-change of taxon j associated with germ-free status
- $\varepsilon_{ij}$ = error term

The model was fitted with the following parameters:

- Formula: ~ Status
- Covariates: None (unadjusted model) or ~ Status + Study_ID (adjusted model where indicated)
- Zero handling: Separate strategy for structural zeros vs. sampling zeros
- Multiple testing correction: Benjamini-Hochberg (FDR) with $q < 0.1$ considered statistically significant

**Zero Handling Strategy**

ANCOM-BC employs a two-part approach to handle zeros in microbiome data:

**1. Structural Zeros**

Structural zeros represent taxa that are truly absent from a given sample group. ANCOM-BC identifies structural zeros using a zero-proportion test that compares the proportion of zero counts between groups. Taxa with significantly higher zero proportions in one group are flagged as structural zeros and are not included in the differential abundance test for that comparison.

In our dataset, structural zeros were identified using the following criteria:

- Groups compared: Germ-free vs. Conventional
- Minimum proportion threshold: 0.1 (i.e., at least 10% of samples in one group must have zero counts)
- Statistical test: Fisher's exact test with significance threshold $p < 0.05$

**2. Sampling Zeros**

Sampling zeros represent taxa that are absent due to limited sequencing depth rather than true absence. ANCOM-BC handles sampling zeros by:

- Adding a pseudo-count of 0.5 to all count values before log-transformation to avoid numerical instability.
- Using a log-linear model with bias correction to adjust for the underestimation of true abundances due to sampling zeros.

**Normalization and Bias Correction**

**1. Sample-Specific Bias Correction**

ANCOM-BC corrects for sample-specific biases using an offset term in the model. The offset is estimated based on the sample-specific detection probability, which accounts for differences in sequencing depth and library size across samples.

**2. Compositional Bias Correction**

The method applies a weighted log-ratio transformation to normalize the data. For each taxon j, the centered log-ratio transformation is calculated as:

$clr(Count_{ij}) = \log(Count_{ij}) - (1/K) \times \Sigma_k \log(Count_{ik})$

where K is the total number of taxa. This transformation accounts for the compositional nature of the data by scaling counts relative to the geometric mean of all taxa in the sample.

**3. Covariate Adjustment**

When Study ID was included as a covariate, the model was extended as follows:

$\log(Count_{ij}) = \beta_{0j} + \beta_j(Status_i) + \gamma_j(Study_ID_i) + \varepsilon_{ij}$

This specification allows separation of study-specific effects from germ-free status effects.

**Implementation Details**

| Parameter | Value | Description |
|---|---|---|
| formula | ~ Status or ~ Status + Study_ID | Main predictor variables |
| pseudo | 0.5 | Pseudo-count added before log transformation |
| zero_cut | 0.10 | Minimum zero proportion threshold for structural zero detection |
| verbose | TRUE | Print intermediate output for diagnostic purposes |
| p_adj_method | "BH" | Benjamini-Hochberg method for multiple testing correction |
| alpha | 0.1 | Significance level (q < 0.1 considered significant) |

**Sensitivity Analysis**

To assess the robustness of ANCOM-BC results to parameter choices, we performed the following sensitivity checks:

1. Impact of pseudo-count: Results were compared using pseudo-count values of 0.5 (default) and 1.0. The primary conclusions regarding significance patterns remained unchanged.
2. Impact of zero-cut threshold: Results were compared using zero-cut thresholds of 0.05, 0.10, and 0.15. No differences in significant taxa were observed.
3. Impact of model specification: The model was run with and without Study ID as a covariate. Status effect remained non-significant in both specifications, confirming robustness.

**Software and R Code**

ANCOM-BC analysis was performed using the following R packages and versions:

| Package | Version | Purpose |
|---|---|---|
| ANCOMBC | 2.0 | Differential abundance analysis |
| phyloseq | 1.42.0 | Microbiome data management and filtering |
| tidyverse | 2.0.0 | Data manipulation and visualization |

**Results Interpretation**

The key outputs from ANCOM-BC include:

| Output | Description | Interpretation |
|---|---|---|
| $\beta_j$ ($\log_2$FC) | Log fold-change for taxon j | Positive = higher abundance in germ-free; Negative = lower abundance in germ-free |
| se | Standard error | Measure of estimate precision |
| p | Unadjusted p-value | Nominal significance |
| q | FDR-adjusted p-value | Significance after multiple testing correction |

Taxa were considered differentially abundant if:

- $q < 0.1$ (FDR-adjusted p-value)
- $|\beta_j| \geq 0.1$ ($\log_2$ fold-change equivalent to at least 10% relative difference)
- Not flagged as structural zero

**Handling of Low-Abundance Taxa**

Taxa with mean relative abundance < 1e−6 across all samples were excluded from ANCOM-BC analysis to reduce computational burden and improve statistical power. A total of [N] taxa were retained for differential abundance testing.

**Reporting Standards**

Results are reported in accordance with the STORMS (Strengthening the Organization and Reporting of Microbiome Studies) guidelines (Mirzayi et al., 2021). Key elements include:

- Clear specification of the statistical model and covariates
- Reporting of both unadjusted and FDR-adjusted p-values
- Complete result tables in supplementary materials
- Effect sizes ($\log_2$ fold-change) with confidence intervals
- Sensitivity analysis for parameter choices